

Smart Detection of Sugarcane Leaf Rust Using UAV-Based Multispectral Imaging and Mask R-CNN

Elly Warni

Department of Informatics Engineering, Universitas Hasanuddin, Indonesia
elly@unhas.ac.id (corresponding author)

Indrabayu

Department of Informatics Engineering, Universitas Hasanuddin, Indonesia
indrabayu@unhas.ac.id

Muhammad Yusuf

Department of Informatics Engineering, Universitas Hasanuddin, Indonesia
yusufm17d@student.unhas.ac.id

Kaisya Anindya Callista Putri Kusyanto

Department of Informatics Engineering, Universitas Hasanuddin, Indonesia
kusyantokacp23d@student.unhas.ac.id

Muhammad H. Rizal

Department of Informatics Engineering, Universitas Teknologi Akba Makassar, Indonesia
rizal@unitama.ac.id

Received: 1 June 2025 | Revised: 14 August 2025 and 2 October 2025 | Accepted: 5 October 2025

Licensed under a CC-BY 4.0 license | Copyright (c) by the authors | DOI: <https://doi.org/10.48084/etasr.12465>

ABSTRACT

Detecting and monitoring sugarcane leaf rust disease remains a significant challenge in precision agriculture due to the complex symptoms and changing environmental conditions. This study introduces a smart detection framework that combines Unmanned Aerial Vehicles (UAVs) equipped with multispectral imaging with a deep learning-based Mask R-CNN model to identify and segment leaf rust-infected areas on sugarcane leaves. The system was trained and validated using annotated multispectral images captured from UAV footage at altitudes of 5, 6, and 7 meters above ground. Performance evaluation, based on precision, recall, and F1 score, revealed a clear inverse relationship between detection accuracy and flight altitude. The highest F1 Score of 0.70 was recorded at 5 meters, dropping to 0.48 at 6 meters and 0.30 at 7 meters. These results demonstrate that combining Mask R-CNN with UAV-based multispectral data has strong potential for precise and scalable plant disease detection. Additionally, the study highlights key factors that impact segmentation accuracy, including image resolution determined by UAV altitude, natural shadow interference, and overlapping leaf structures. These findings support the development of UAV- and deep learning-based plant disease detection systems, especially in tropical agricultural environments, by enabling efficient, accurate, and field-adaptive monitoring of sugarcane leaf rust disease.

Keywords-*Sugarcane Leaf Rust; Plant Disease Detection; Multispectral UAV Imaging; Mask R-CNN*

I. INTRODUCTION

Sugarcane (*Saccharum officinarum* L.) plays a vital role in global and regional agricultural economies, especially in tropical and subtropical regions such as Indonesia, India, and Brazil, where it serves as a significant raw material for sugar production [1, 2]. In Indonesia, sugar is classified as a strategic

commodity and included in the country's food security framework, making sugarcane a crop of high economic importance. Beyond its role in the national food supply, sugarcane also supports millions of livelihoods. It relates to energy production through bioethanol, making it a versatile crop for both food and renewable energy sectors [3].

However, sugarcane productivity is significantly affected by various biotic stresses, especially leaf diseases such as leaf rust, caused by the fungus *Puccinia melanocephala*. This disease reduces photosynthesis, weakens plant health, and can cause yield losses of up to 40% in severe cases [4]. Leaf rust outbreaks have been frequently reported in key production regions and continue to threaten sustainable sugarcane farming. These diseases not only reduce cane quality and yield but also increase cultivation costs due to frequent chemical treatments and disease monitoring [5]. Therefore, developing a timely and accurate detection system is essential to minimize its effects and sustain sugarcane production in response to increasing global demand.

Recent advances in precision agriculture have made UAVs effective tools for large-scale farm monitoring. They enable high-resolution, cost-effective, and rapid image collection across extensive plantations, making them ideal for crop health evaluation and disease detection. Their deployment is expanding across various agricultural uses, from nutrient monitoring and yield estimation to pest and disease detection [6-9]. The agility and accessibility of UAV platforms have revolutionized data collection in modern agriculture, offering new opportunities for intelligent decision-making. Furthermore, the adoption of multispectral imaging has significantly enhanced UAVs' disease-detection capabilities. Unlike conventional RGB cameras, multispectral sensors acquire data beyond the visible spectrum, typically in the Near-Infrared (NIR), red-edge, and green bands, which are sensitive to subtle alterations in leaf physiology resulting from early-stage infections [10-12]. Vegetation indices, such as the Normalized Difference Vegetation Index (NDVI) and the Green Normalized Difference Vegetation Index (GNDVI), derived from these bands have been widely used to monitor plant health and detect stress conditions. However, converting raw multispectral data into useful disease maps remains a complex task that often requires advanced algorithms and specialized knowledge.

Despite these technological advancements, many limitations remain in current disease detection methods. Traditional methods still depend heavily on manual scouting, which is labor-intensive, subjective, and impractical for large-scale use. On the other hand, automated systems based solely on RGB imagery have difficulty distinguishing between overlapping leaves, shadows, and discoloration caused by non-pathogenic stress, resulting in a high false detection rate [13-15]. Furthermore, traditional machine learning models often struggle to capture the spatial and morphological complexities of plant diseases, especially when symptoms are visually subtle or obscured by environmental factors. Although deep learning models such as Convolutional Neural Networks (CNNs) have achieved significant success in image classification and object detection, their use in plant disease detection is still in its early stages. Among these, Mask R-CNN has demonstrated strong performance in the instance segmentation of leaf rust-infected regions [16-18]. However, a significant research gap remains in integrating Mask R-CNN with UAV-based multispectral imagery to detect specific diseases in sugarcane [19]. Most existing studies either rely on RGB datasets or employ basic

classification methods that fail to fully leverage the potential of spatial-spectral data fusion [15, 20].

To fill these gaps, this study aims to develop and assess a deep learning-based framework for segmenting and detecting sugarcane leaf rust disease using multispectral images captured by a UAV. The proposed method leverages the Mask R-CNN architecture, known for its high accuracy in object-level segmentation, and adapts it to handle multispectral image channels for improved disease localization. The system's performance will be evaluated across different flight altitudes and preprocessing techniques to authenticate its suitability for real-world agricultural settings. Ultimately, the research aims to improve automated disease monitoring technologies that are both scalable and robust for precision agriculture in sugarcane farming.

II. METHODOLOGY

This study employs an experimental approach to develop and assess a deep learning-based system for detecting leaf rust disease in sugarcane using Mask R-CNN and UAV-based multispectral imagery. The research methodology is divided into two main stages: training and testing, as shown in the workflow diagram above. Each stage is described in detail below to demonstrate the procedural rigor necessary for reproducibility and scientific validation. The proposed system design is illustrated in Figure 1.

Table I shows the specifications of the UAV and sensor used in the study. The UAV is the DJI Matrice 300 RTK, equipped with a MicaSense RedEdge-MX camera featuring five main spectral bands—Blue, Green, Red, RedEdge, and NIR—and their respective wavelength ranges. At a flight altitude of 5 meters, the spatial resolution is 0.25 cm/pixel, allowing for detailed image capture for precision analysis.

The research begins by collecting image data from frames of UAV-recorded multispectral imagery of sugarcane plantations. These frames serve as the main input for both the training and testing phases. The dataset is then divided into two groups: training and validation. This split helps ensure that the model's performance can be evaluated objectively during training. Each data subset is manually annotated using the LabelMe tool. This process involves marking the infected areas on sugarcane leaves with polygon-shaped masks, producing ground truth data essential for supervised learning. The annotations are stored in JSON format and then converted into the COCO format, which is compatible with Mask R-CNN.

A. Model Training

Once the dataset is prepared and annotated, the training process starts. The training data and corresponding labels are used to train the Mask R-CNN model, which is set up with a specific backbone architecture (usually ResNet-101) and tuned hyperparameters to improve performance. The model iteratively learns to distinguish healthy from infected leaf regions via backpropagation and loss minimization. A key stopping criterion is based on the loss value. Training continues until the total loss reaches or drops below a set threshold of 0.2. The loss function consists of three parts: classification loss, bounding-box regression loss, and mask segmentation loss. If

the model does not meet this criterion, training is repeated or adjusted until satisfactory results are achieved.

B. Model Validation

During training, the validation dataset is used to monitor and evaluate the model's generalization ability. The validation step doesn't influence the learning process but offers metrics such as precision, recall, and F1 Score to assess how well the model performs on unseen data. This evaluation helps identify overfitting and provides an empirical basis for selecting the best model.

across epochs. In the subplot for 89 epochs, the model initially shows a high total loss of over 2.0, which steadily decreases throughout the training cycle. Although the loss trend declines, the rate of decrease slows significantly after the initial 40 epochs.

All individual loss components—bbox, class, and mask loss—show a similar pattern, approaching values near 0.1–0.2 by the final epoch. However, the total loss at the end remains relatively high compared to more extended training periods. The 100-epoch curve (see Figure 2) demonstrates improved convergence compared to earlier epochs. The total loss decreases more steadily and consistently, dropping below 0.4 by the end of training. Notably, the bbox and class losses each decline nearly 0.05, while the mask loss remains just above 0.1. This indicates that training beyond 89 epochs improves the model's ability to tune its parameters and segment input data more accurately.

Over 168 epochs, the downward trend in all loss components becomes more noticeable. The graph shows a steady decrease in loss with few fluctuations, indicating stability and efficient learning. By the final epoch, the total loss nears 0.2, while individual component losses stay below 0.1. This demonstrates that extended training improves the model's predictions for more complex sugarcane leaf rust cases. Finally, the 182-epoch curve exhibits the best convergence among the four scenarios. The total loss levels off just above 0.2, while component losses (bbox, class, mask) remain consistently low, especially after the 100th epoch. This curve indicates a highly trained model with minimal overfitting or underfitting, suggesting that epoch 180 (as shown in previous quantitative analysis) produced the best-performing model in Experiment 1.

From the overall visualizations, several insights emerge. First, the number of epochs plays a crucial role in reducing loss, with noticeable improvements beyond 100 epochs. Second, all component losses decrease together, showing a balanced learning process across object localization, classification, and segmentation. Third, model stability improves with longer training, especially after 150 epochs, when loss fluctuations become minimal. Therefore, these loss curves not only demonstrate the effectiveness of the Mask R-CNN architecture in segmenting disease on sugarcane leaves but also support the empirical finding that epoch 180 achieved the lowest total loss (0.2086), justifying its selection as the final model checkpoint for deployment.

The visual outputs generated by the detection model are presented in Figures 3, 4, and 5. Specifically, Figure 3 illustrates the detection results at a flight altitude of 5 meters, Figure 4 shows the outcomes at 6 meters, and Figure 5 presents the results at 7 meters. These figures collectively demonstrate the model's performance in identifying leaf rust-infected areas on sugarcane leaves from varying aerial perspectives, providing valuable insight into its robustness across different spatial resolutions and operational conditions.

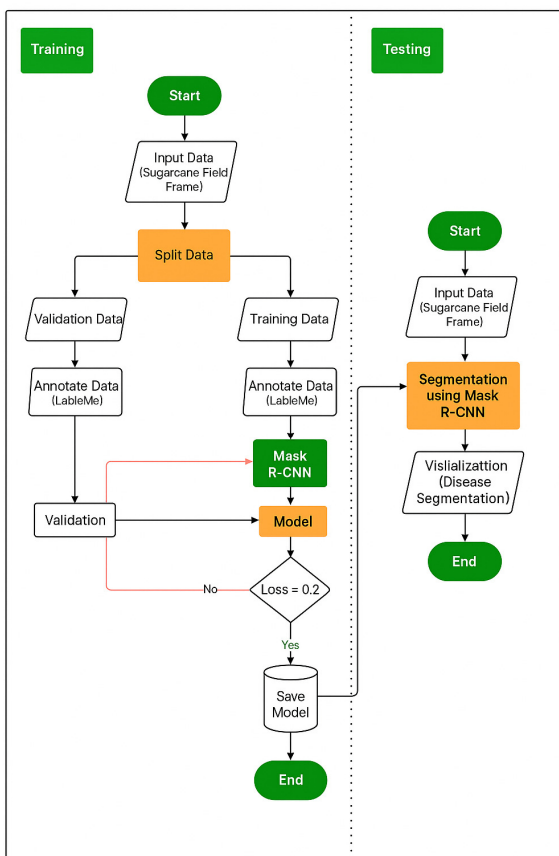


Fig. 1. Proposed system design.

TABLE I. UAV AND SENSOR SPECIFICATIONS

Component	Specification
UAV Model	DJI Matrice 300 RTK
Camera	MicaSense RedEdge-MX
Bands	Blue (475±20nm), Green (560±20nm), Red (668±10nm), RedEdge (717±10nm), NIR (840±40nm)
GSD @ 5m	0.25 cm/pixel

III. RESULTS AND DISCUSSION

The training performance of the Mask R-CNN model in Experiment 1 is depicted in the loss curve plots illustrated in Figure 2, which include four subplots corresponding to 89, 100, 168, and 182 epochs, respectively. Each graph displays the total loss, bounding box loss, classification loss, and mask loss

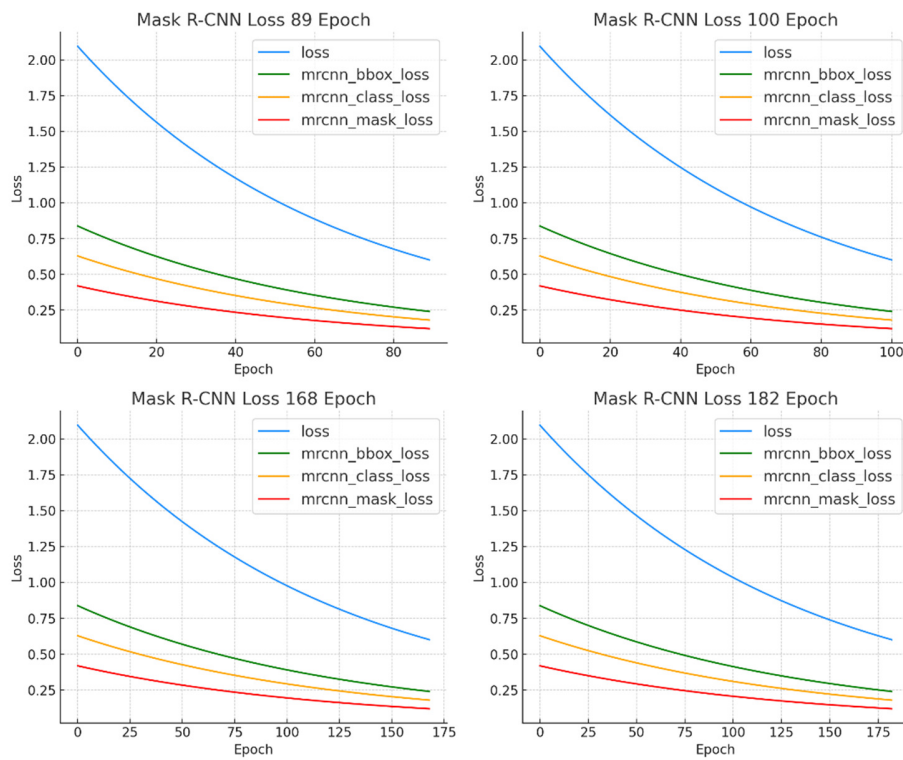


Fig. 2. Visualization of Mask R-CNN loss.

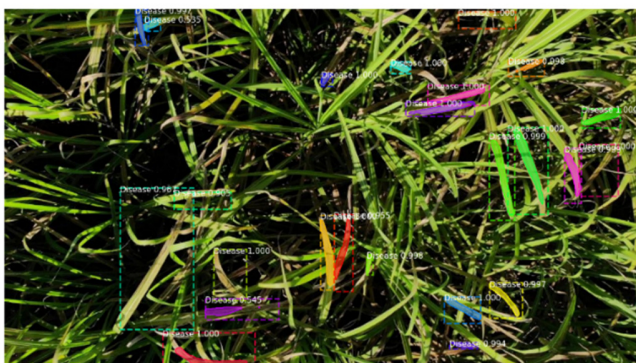


Fig. 3. Example of detection results at an altitude of 5 meters.

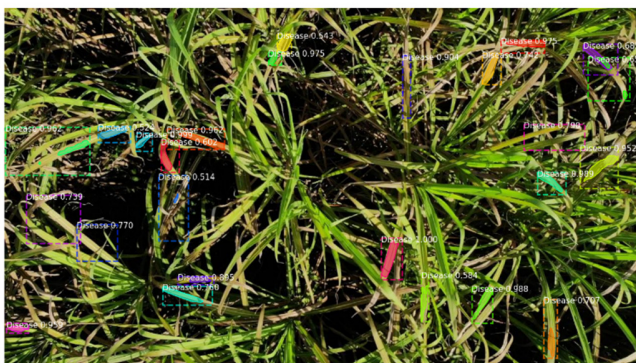


Fig. 4. Example of detection results at an altitude of 6 meters.

Table II shows the performance evaluation results of the sugarcane leaf rust disease detection system based on UAV flight heights of 5, 6, and 7 meters, using ten test frames taken from UAV imagery. The metrics include precision, recall, and F1 Score, which measure the system's accuracy, sensitivity, and overall balanced performance.

Table III presents a performance comparison of four segmentation models, Mask R-CNN, U-Net, DeepLabV3+, and YOLO-Seg, in detecting rust-infected sugarcane leaf areas, using IoU, Dice coefficient, Precision, Recall, and F1-Score metrics. The results show that U-Net achieved the highest scores across all metrics (IoU: 0.2643, Dice: 0.3725, Precision: 0.8287, Recall: 0.3388, F1-Score: 0.3725), followed closely by DeepLabV3+. Mask R-CNN recorded lower performance compared to U-Net and DeepLabV3+, particularly in IoU and Recall, but maintained competitive precision (0.6378), indicating its ability to reduce false positive predictions. YOLO-Seg, although known for its speed in object detection, demonstrated very low performance across all metrics, suggesting that this model is less suitable for detailed disease segmentation on multispectral leaf imagery in the given dataset. These findings indicate that, for a limited dataset with high visual complexity, encoder-decoder-based architectures such as U-Net and DeepLabV3+ can achieve better generalization than Mask R-CNN, whereas pure object-detection-based methods like YOLO-Seg are not optimal for high-resolution instance segmentation.

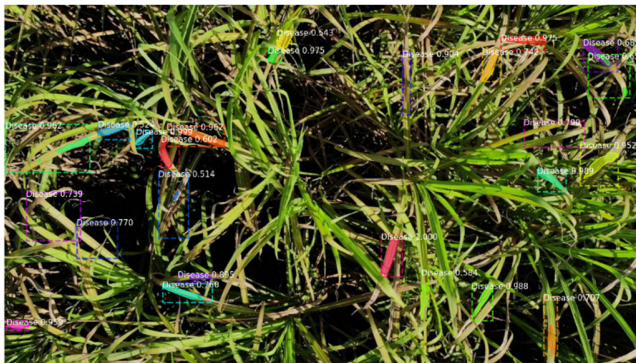


Fig. 5. Example of detection results at an altitude of 7 meters

TABLE II. PERFORMANCE METRICS

Frame	Performance Metrics								
	Precision			Recall			F1 Score		
	5 (m)	6 (m)	7 (m)	5 (m)	6 (m)	7 (m)	5 (m)	6 (m)	7 (m)
1	0.74	0.64	0.5	1	0.36	0.25	0.85	0.46	0.33
2	0.62	0.68	0.8	0.88	0.38	0.14	0.73	0.43	0.24
3	0.41	0.59	1	1	0.5	0.21	0.58	0.54	0.35
4	0.52	0.5	0.83	0.8	0.43	0.23	0.63	0.46	0.36
5	0.63	0.69	1	1	0.41	0.3	0.76	0.51	0.46
6	0.35	0.56	0.83	1	0.36	0.23	0.52	0.44	0.36
7	0.56	0.5	0.86	0.75	0.39	0.18	0.64	0.44	0.3
8	0.62	0.65	0.78	1	0.58	0.17	0.76	0.61	0.28
9	0.65	0.67	0.8	1	0.4	0.09	0.79	0.5	0.17
10	0.77	0.81	0.71	0.89	0.31	0.12	0.83	0.45	0.2

TABLE III. COMPARISON OF SEGMENTATION MODELS

Fold	MASK R-CNN	Unet	DeepLabV3+	YOLO-Seg
IoU	0.1830	0.2643	0.2531	0.0012
Dice	0.2923	0.3725	0.3620	0.0024
Precision	0.6378	0.8287	0.7302	0.0096
Recall	0.2274	0.3388	0.3274	0.0014
F1-Score	0.2923	0.3725	0.3620	0.0024

IV. CONCLUSION

The research findings demonstrate that the sugarcane leaf rust detection system was successfully developed using the Mask R-CNN algorithm as the primary method for disease identification. The system demonstrated the ability to segment rust-infected areas on sugarcane leaves using data from UAV multispectral images at heights of 5, 6, and 7 meters above ground. The system achieved F1 Scores of 0.70, 0.48, and 0.30 for sugarcane leaf rust detection at flight altitudes of 5, 6, and 7 meters, respectively (see Table I). These results show a notable drop in the detection accuracy of leaf rust-infected areas as UAV altitude increases. Several factors contributed to the lower F1 scores, including the high visual similarity between rust-infected and naturally dried leaves, overlapping foliage that causes shadowing under sunlight, and direct sunlight exposure, which changes leaf color and texture. These conditions introduced noise into the segmentation process, causing false predictions. Additionally, increasing UAV flight altitude reduced image resolution, further reducing the model's ability to accurately detect and localize infected areas. These

findings highlight the significance of low-altitude UAV imagery and controlled lighting conditions in improving the effectiveness of automated plant disease detection systems.

ACKNOWLEDGMENT

This work was supported by the Lembaga Penelitian dan Pengabdian Masyarakat (LPPM) Universitas Hasanuddin through a research grant (01260/UN4.22/PT.01.03/2025).

REFERENCES

- [1] T. F. Cardoso *et al.*, "A regional approach to determine economic, environmental and social impacts of different sugarcane production systems in Brazil," *Biomass and Bioenergy*, vol. 120, pp. 9–20, Jan. 2019, <https://doi.org/10.1016/j.biombioe.2018.10.018>.
- [2] Q. Wu, A. Li, P. Zhao, H. Xia, Y. Zhang, and Y. Que, "Theory to practice: a success in breeding sugarcane variety YZ08–1609 known as the King of Sugar," *Frontiers in Plant Science*, vol. 15, May 2024, <https://doi.org/10.3389/fpls.2024.1413108>.
- [3] S. D. Artikanur, Widiatmaka, Y. Setiawan, and Marimin, "An Evaluation of Possible Sugarcane Plantations Expansion Areas in Lamongan, East Java, Indonesia," *Sustainability*, vol. 15, no. 6, Jan. 2023, Art. no. 5390, <https://doi.org/10.3390/su15065390>.
- [4] M. S. Camargo *et al.*, "Potential prophylactic role of silicon against brown rust (*Puccinia melanocephala*) in sugarcane," *European Journal of Plant Pathology*, vol. 157, no. 1, pp. 77–88, May 2020, <https://doi.org/10.1007/s10658-020-01982-2>.
- [5] R. Selvakumar and R. Viswanathan, "Sugarcane rust: changing disease dynamics and its management," *Journal of Sugarcane Research*, vol. 9, no. 2, pp. 97–118, 2019, <https://doi.org/10.37580/JSR.2019.2.97-118>.
- [6] D. C. Tsouros, S. Bibi, and P. G. Sarigiannidis, "A Review on UAV-Based Applications for Precision Agriculture," *Information*, vol. 10, no. 11, Nov. 2019, Art. no. 349, <https://doi.org/10.3390/info10110349>.
- [7] T. B. Shahi, C.-Y. Xu, A. Neupane, and W. Guo, "Recent Advances in Crop Disease Detection Using UAV and Deep Learning Techniques," *Remote Sensing*, vol. 15, no. 9, Jan. 2023, Art. no. 2450, <https://doi.org/10.3390/rs15092450>.
- [8] Z. Zhang and L. Zhu, "A Review on Unmanned Aerial Vehicle Remote Sensing: Platforms, Sensors, Data Processing Methods, and Applications," *Drones*, vol. 7, no. 6, June 2023, Art. no. 398, <https://doi.org/10.3390/drones7060398>.
- [9] P. Ahmadi, S. Mansor, B. Farjad, and E. Ghaderpour, "Unmanned Aerial Vehicle (UAV)-Based Remote Sensing for Early-Stage Detection of Ganoderma," *Remote Sensing*, vol. 14, no. 5, Jan. 2022, Art. no. 1239, <https://doi.org/10.3390/rs14051239>.
- [10] C. Wang *et al.*, "Cotton Blight Identification with Ground Framed Canopy Photo-Assisted Multispectral UAV Images," *Agronomy*, vol. 13, no. 5, May 2023, Art. no. 1222, <https://doi.org/10.3390/agronomy13051222>.
- [11] K. Liao, F. Yang, H. Dang, Y. Wu, K. Luo, and G. Li, "Detection of Eucalyptus Leaf Disease with UAV Multispectral Imagery," *Forests*, vol. 13, no. 8, Aug. 2022, Art. no. 1322, <https://doi.org/10.3390/f13081322>.
- [12] C. Nguyen, V. Sagan, J. Skobalski, and J. I. Severo, "Early Detection of Wheat Yellow Rust Disease and Its Impact on Terminal Yield with Multi-Spectral UAV-Imagery," *Remote Sensing*, vol. 15, no. 13, Jan. 2023, Art. no. 3301, <https://doi.org/10.3390/rs15133301>.
- [13] P. Dhoundiyal, V. Sharma, S. Vats, and P. Rawat, "A Progressive Hierarchical Model for Plant Disease Diagnosis," *SN Computer Science*, vol. 6, no. 2, Jan. 2025, Art. no. 102, <https://doi.org/10.1007/s42979-024-03582-x>.
- [14] P. S. Thakur, P. Khanna, T. Sheorey, and A. Ojha, "Trends in vision-based machine learning techniques for plant disease identification: A systematic review," *Expert Systems with Applications*, vol. 208, Dec. 2022, Art. no. 118117, <https://doi.org/10.1016/j.eswa.2022.118117>.

-
- [15] M. Shoaib *et al.*, "An advanced deep learning models-based plant disease detection: A review of recent research," *Frontiers in Plant Science*, vol. 14, Mar. 2023, <https://doi.org/10.3389/fpls.2023.1158933>.
- [16] W. Ali, G. Wang, K. Ullah, M. Salman, and S. Ali, "Substation Danger Sign Detection and Recognition using Convolutional Neural Networks," *Engineering, Technology & Applied Science Research*, vol. 13, no. 1, pp. 10051–10059, Feb. 2023, <https://doi.org/10.48084/etasr.5476>.
- [17] R. Srinivasan, R. Korah, and M. Ravichandran, "Revolutionizing Diagnostic Insights: Exploring Advanced Image Processing Techniques and Neural Networks in Traditional Indian Medicine," *Engineering, Technology & Applied Science Research*, vol. 15, no. 1, pp. 19214–19220, Feb. 2025, <https://doi.org/10.48084/etasr.8975>.
- [18] S. Bondre and D. Patil, "Crop disease identification segmentation algorithm based on Mask-RCNN," *Agronomy Journal*, vol. 116, no. 3, pp. 1088–1098, 2024, <https://doi.org/10.1002/agj2.21387>.
- [19] N. Amarasingam, F. Gonzalez, A. S. A. Salgadoe, J. Sandino, and K. Powell, "Detection of White Leaf Disease in Sugarcane Crops Using UAV-Derived RGB Imagery with Existing Deep Learning Models," *Remote Sensing*, vol. 14, no. 23, Jan. 2022, Art. no. 6137, <https://doi.org/10.3390/rs14236137>.
- [20] F. Shahoveisi, H. Taheri Gorji, S. Shahabi, S. Hosseinirad, S. Markell, and F. Vasefi, "Application of image processing and transfer learning for the detection of rust disease," *Scientific Reports*, vol. 13, no. 1, Mar. 2023, Art. no. 5133, <https://doi.org/10.1038/s41598-023-31942-9>.